ANTIMICROBIAL AGENTS AND CHEMOTHERAPY, May 2010, p. 2152–2159 Vol. 54, No. 5
0066-4804/10/$12.00 doi:10.1128/AAC.01315-09

Antiviral Activity of a Small-Molecule Inhibitor of Filovirus Infection▽

Travis K. Warren,[1] Kelly L. Warfield,[1]† Jay Wells,[1] Sven Enterlein,[2] Mark Smith,[1] Gordon Ruthel,[1] Abdul S. Yunus,[3] Michael S. Kinch,[3]* Michael Goldblatt,[3] M. Javad Aman,[2] and Sina Bavari[1]*

U.S. Army Medical Research Institute of Infectious Diseases, Fort Detrick, Frederick, Maryland[1]; Integrated BioTherapeutics, Inc., Germantown, Maryland[2]; and Functional Genetics, Inc., Gaithersburg, Maryland[3]

Received 17 September 2009/Returned for modification 21 October 2009/Accepted 24 February 2010

There exists an urgent need to develop licensed drugs and vaccines for the treatment or prevention of filovirus infections. FGI-103 is a low-molecular-weight compound that was discovered through an *in vitro* screening assay utilizing a variant of *Zaire ebolavirus* (ZEBOV) that expresses green fluorescent protein. *In vitro* analyses demonstrated that FGI-103 also exhibits antiviral activity against wild-type ZEBOV and *Sudan ebolavirus*, as well as *Marburgvirus* (MARV) strains Ci67 and Ravn. *In vivo* administration of FGI-103 as a single intraperitoneal dose of 10 mg/kg delivered 24 h after infection is sufficient to completely protect mice against a lethal challenge with a mouse-adapted strain of either ZEBOV or MARV-Ravn. In a murine model of ZEBOV infection, delivery of FGI-103 reduces viremia and the viral burden in kidney, liver, and spleen tissues and is associated with subdued and delayed proinflammatory cytokine responses and tissue pathology. Taken together, these results identify a promising antiviral therapeutic candidate for the treatment of filovirus infections.

Members of the genera *Ebolavirus* (EBOV) and *Marburgvirus* (MARV) make up the family *Filoviridae* and are causative agents responsible for severe hemorrhagic fever. Currently, five EBOV species are recognized: *Zaire ebolavirus* (ZEBOV), *Sudan ebolavirus* (SEBOV), *Côte d'Ivoire ebolavirus*, *Reston ebolavirus*, and "*Bundibugyo ebolavirus*." ZEBOV and SEBOV are the etiologic agents responsible for outbreaks of Ebola hemorrhagic fever (EHF) that impact humans and nonhuman primates in regions of endemicity in sub-Saharan Africa (13). In humans, case fatality rates range from 50 to 90% for ZEBOV, which is considered the most virulent of EBOV species (13). A single species of MARV (*Lake Victoria marburgvirus*) causes Marburg hemorrhagic fever (MHF) among humans and nonhuman primates. Case fatality rates of up to 90% have been reported for outbreaks (6, 13). Isolated cases of MHF and EHF have occurred as a result of laboratory work involving nonhuman primate species imported from regions of endemicity, through accidental needle stick injuries of laboratory workers (12), and through travel by individuals unknowingly exposed in regions of endemicity (20). Currently, there are no therapies or preventative vaccines licensed for use to treat filovirus infections.

Targeting host processes provides a promising approach for antiviral therapeutic development efforts to combat filoviruses. Both EBOV and MARV encode a limited number of viral products and rely on numerous host processes in order to successfully enter cells, replicate genomic material, assemble infectious virions, and ultimately exit from infected cells. By targeting host processes many different viral pathogens utilize during infection, potential opportunities arise to develop agents with broad-spectrum antiviral activity (7, 19). Another potential advantage to this approach is that by targeting host processes, it will likely prove difficult for viruses to switch to alternative pathways by tolerable individual-base mutations, thus limiting the potential amplification of drug-resistant variants.

Here we report on the identification of a nonpeptidic small molecule, designated FGI-103, discovered via a high-throughput screen designed to detect inhibitors of EBOV. Further evaluations have shown FGI-103 to exhibit potent antiviral activity against all of the strains of EBOV and MARV tested thus far. Additionally, we describe results from *in vivo* investigations demonstrating that a single dose of FGI-103 protects mice against lethal challenges with either MARV or EBOV in a therapeutic scenario.

MATERIALS AND METHODS

Compound libraries. Multiple compound libraries were obtained from the National Cancer Institute (NCI, Frederick, MD). Compounds in these libraries shared chemical scaffolds composed of one or two heterocyclic aromatic structures (i.e., indole, benzofuran, benzimidazole, or benzothiophene) connected via an aliphatic linker or directly to a phenyl substituent and possessing two positive-ionizable amidine or imidazolino moieties. The antiviral activity of FGI-103 (Fig. 1) against ZEBOV was discovered through a screening of these NCI libraries. Custom synthesis of additional lots of compound was conducted either by Combinix, Inc. (Mountain View, CA), or Recirca, Inc. (Painesville, OH).

EBOV screening assay. Vero E6 cells were plated in 96-well tissue culture plates and grown to confluence. Prior to viral infection, cells were pretreated overnight with compounds diluted from 10 mM dimethyl sulfoxide (DMSO) stocks to a concentration of 20 μM in 100 μl of Eagle's minimum essential medium (EMEM) containing 10% fetal bovine serum (FBS). Cells were infected at a multiplicity of infection (MOI) of 1 with a strain of EBOV-Zaire (ZEBOV) that expresses green fluorescent protein (GFP) (ZEBOV-GFP) (21). Virus was added to cells in 100 μl of EMEM containing 10% FBS. After 1 h, excess virus was removed and EMEM containing 10% FBS and a test compound (at a concentration of 20 μM) was added to the treatment wells. After a 48-h incubation period, cells were fixed with 10% neutral-buffered formalin for 3 days and cell nuclei were labeled with Hoechst dye. To determine the percentage of

* Corresponding author. Mailing address for Michael Kinch: 708 Quince Orchard Road, Gaithersburg, MD 20882. Phone: (240) 631-6799. Fax: (240) 631-6794. E-mail: mkinch@functional-genetics.com. Mailing address for Sina Bavari: 1425 Porter Street, Fort Detrick, MD 21702. Phone: (301) 619-4246. Fax: (541) 754-3545. E-mail: sina.bavari@us.army.mil.

† Present address: Integrated BioTherapeutics, Inc. (IBT), 20358 Seneca Meadows Parkway, Germantown, MD 20876.

▽ Published ahead of print on 8 March 2010.

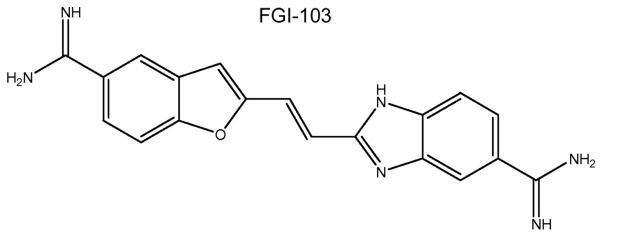

2-(2-(5-(amino(imino)methyl)-1-benzofuran-2-yl)vinyl)-1H-benzimidazole-5-carboximidamide

FIG. 1. Chemical structure of FGI-103.

GFP-expressing cells, plates were analyzed using a Discovery-1 automated microscope (Molecular Devices Corp., Sunnyvale, CA). GFP expression was quantified in each well from nine individual locations containing approximately 2,000 cells per location. Within each experiment, triplicate wells were examined for each treatment condition. Percent inhibition values were calculated as follows: $100 \times [1 - (\text{average GFP fluorescence from compound-treated wells/average fluorescence from wells containing medium only})]$.

In vitro inhibition assay. Confluent monolayers of Vero E6 cells were pretreated overnight with FGI-103 diluted to various concentrations in EMEM containing 10% FBS. FGI-103 was diluted from a 10 mM DMSO stock using a dilution scheme that resulted in a 0.5% DMSO concentration in all treatments. Cells were infected for 1 h at an MOI of 1 with EBOV or MARV diluted in EMEM containing 10% FBS. Excess virus was removed, and medium containing FGI-103 at concentrations equivalent to pretreatment concentrations and 0.5% DMSO was added to the cells, which were then incubated for 48 h. Supernatant was harvested and subjected to a plaque reduction assay using Vero E6 cells. Percent inhibition was calculated as follows: $100 \times [1 - (\text{viral titer of treatment wells/viral titer of negative-control wells})]$.

In vitro cytotoxicity assay. The 50% cytotoxic concentration (CC_{50}) of FGI-103 was determined for a variety of different cell lines, including MDCK, HEp2, Vero E6, HEK-293T, and A549 cells. Confluent cell monolayers (96-well format) were incubated for 72 h following treatment in triplicate with serially diluted FGI-103 at concentrations of 0.0018 to 320 μM. Cytotoxicity was assessed using a CellTiter Glo kit (Promega, Madison, WI) according to the manufacturer's recommended procedure. Luminescence was determined using a Modulus Microplate reader (Turner Biosystems, Sunnyvale, CA).

In vivo filovirus challenge studies. For EBOV experiments, male or female C57BL/6 mice were obtained from the NCI Frederick Cancer Research and Development Center, Frederick, MD. Mice were 8 to 10 weeks of age at the start of each experiment. Animals were housed in microisolator cages and provided autoclaved water and chow *ad libitum*. Standard treatment groups consisted of 10 mice. Mice were challenged intraperitoneally (i.p.) with 1,000 PFU of mouse-adapted EBOV (3). In all experiments, FGI-103 was administered to mice via i.p. delivery in 0.9% saline solution. Animal health and mortality were recorded twice daily for 14 days. Mice that survived for 14 days following the challenge were deemed to be protected. All EBOV-infected animals were handled in a biosafety level 4 (BSL-4) laboratory at the United States Army Medical Research Institute of Infectious Diseases, which is fully accredited by the Association for Assessment and Accreditation of Laboratory Animal Care International. Research was conducted in compliance with the Animal Welfare Act and other federal statutes and regulations relating to animals and experiments involving animals and adhered to principles stated in the Guide for the Care and Use of Laboratory Animals, National Research Council, 1996.

A mouse-adapted strain of MARV-Ravn was used for *in vivo* MARV challenge experiments. The adaptation process involved the serial passage of virus obtained from livers of MARV-infected severe combined immunodeficient mice (23), followed by sequential passage in immunocompetent (BALB/c) mice, which adapted the virus for lethality in both BALB/c and C57BL/6 mice (24). For MARV challenge, male or female BALB/c mice aged 8 to 12 weeks (NCI) were infected by i.p. injection with 1,000 PFU of mouse-adapted MARV-Ravn and the health and survival of the mice were monitored for 14 days following infection. Challenge experiments involving MARV were otherwise conducted under conditions similar to those used for mouse EBOV challenges.

Serum biochemistry and cytokines. Serum samples from individual C57BL/6 mice were frozen at −70°C until all study samples were obtained. Serum samples were analyzed to determine concentrations of alanine aminotransferase (ALT), albumin, alkaline phosphatases (ALP), amylase, aspartate aminotransferase (AST), calcium, creatinine, γ-glutamyltransferase, glucose, total bilirubin, total protein, blood urea nitrogen, and uric acid using a Piccolo Blood Chemistry Analyzer (Abaxis, Union City, CA).

Cytokine analysis of serum was conducted by using a BD Cytometric Bead Array (BD Biosciences, San Jose, CA), according to the manufacturer's instructions.

Viremia, tissue viral loads, and pathology sampling. To evaluate EBOV burdens in mouse organs, animals were euthanized by CO_2 asphyxiation and kidney, spleen, and liver samples were harvested, weighed, and homogenized in cell culture medium. Homogenized tissues were briefly centrifuged, and the supernatant was stored at −80°C. Supernatants and serum were subjected to standard plaque assay using Vero cells.

On days 2, 4, 6, and 8 after EBOV infection, tissues were collected from five mice from a vehicle-control group or from the experimental group treated with 10 mg/kg FGI-103 delivered by i.p. administration 24 h following infection. Tissues were exposed to 10% neutral buffered formalin for a minimum of 30 days under BSL-4 containment, after which tissues were embedded in paraffin. For histological analysis, tissue sections were either stained with hematoxylin and eosin for routine light microscopy or treated with EBOV-specific antisera to identify viral antigen within the tissue samples.

Statistical analysis. Statistical analyses of Kaplan-Meier survival curves were performed using GraphPad Prism software (GraphPad Software, Inc., La Jolla, CA). Pairwise comparisons were conducted using Bonferroni adjustment. Two-way analysis of variance was used to statistically characterize cytokine levels, liver enzyme values, and tissue viral loads (conducted using log-transformed data). For all analyses, comparisons were considered statistically significant at P values of ≤ 0.05.

RESULTS

***In vitro* activity of FGI-103 against EBOV.** To identify inhibitors of EBOV, a small-molecule library was obtained from the NCI and compounds were screened for antiviral activity against ZEBOV-GFP. This particular EBOV variant was selected based on the high pathogenicity associated with the Zaire species, because a rodent model of ZEBOV infection is well established (3), and because the expression of GFP greatly facilitates the detection of compound hits by high-throughput analysis. Using a ZEBOV-GFP assay, 2-(2-(5-(amino(imino)methyl)-1-benzofuran-2-yl)vinyl)-1H-benzimidazole-5-carboximidamide (molecular mass, 453.5 Da), herein designated FGI-103 (Fig. 1), was found to inhibit infection in a dose-dependent manner (Fig. 2).

We considered that ZEBOV-GFP is a recombinant virus and thus confirmed the cell-based efficacy of FGI-103 by using the wild-type virus. Cultured Vero E6 cells were infected with ZEBOV (MOI of 1) in the presence of FGI-103 and incubated for 48 h. The viral titer in culture supernatants was determined using a standard plaque assay. Similar to results obtained for ZEBOV-GFP, FGI-103 exhibited a dose-dependent inhibition of wild-type ZEBOV (Fig. 2). Viral replication was inhibited by >90% in all treatments containing ≥0.8 μM FGI-103. Based on this evaluation, the half-maximal effective concentration (EC_{50}) was found to be 100 nM (EC_{90} of 330 nM). We reasoned that FGI-103 might also demonstrate efficacy against the related SEBOV. Consistent with results obtained for ZEBOV, we observed a dose-dependent inhibition in viral replication assessed using a plaque assay (Fig. 2). The EC_{50} of FGI-103 against SEBOV was calculated as 420 nM (EC_{90} of 960 nM).

To rule out the possibility that FGI-103 was toxic to cells, we evaluated the cytotoxicity of the compound by using the Vero E6, HEK-293T, MDCK, A549, and HEp-2 cell lines and human peripheral blood mononuclear cells. In all of these cell types, the CC_{50} was calculated to be equivalent to or above 50 μM (not shown). Thus, the results generated from these cell-

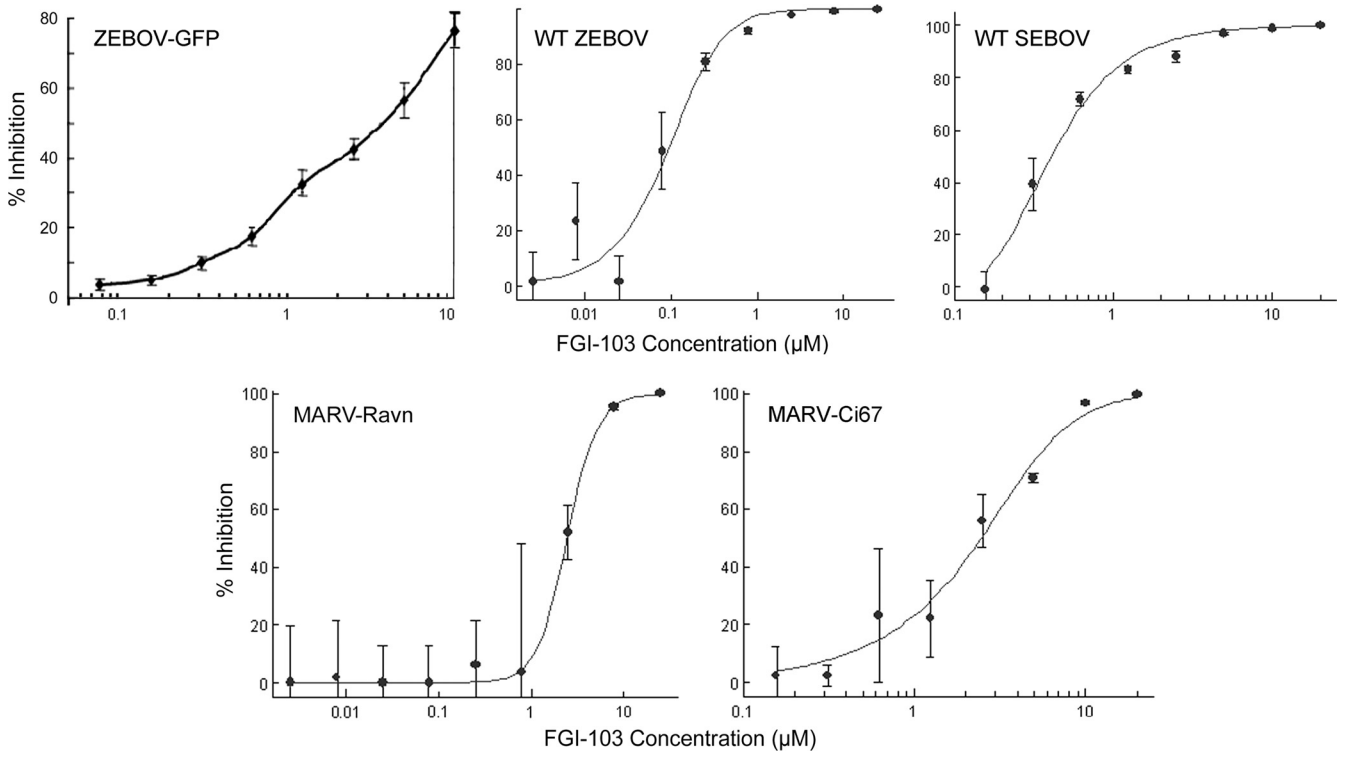

FIG. 2. Inhibition of EBOV by FGI-103. Inhibition of a recombinant strain of ZEBOV that expresses GFP (ZEBOV-GFP) was assessed by pretreating Vero E6 cell monolayers with FGI-103 overnight and for 48 h following infection. Viral yield assays using wild-type (WT) ZEBOV, SEBOV, MARV-Ravn, and MARV-Ci67 were similarly conducted by treating cells with FGI-103 both prior to virus infection (MOI of 1) and for 48 h afterward. Supernatant harvested from treatment wells was subjected to a standard viral plaque assay using Vero E6 cells. For all assays, inhibition is expressed relative to medium-only control wells containing equivalent DMSO concentrations. Error bars represent standard deviations associated with four replicates, except for the ZEBOV-GFP assay, which shows results from three replicates.

based assays likely represent bona fide inhibition of viral replication and are not false-positive observations resulting from cell toxicity.

***In vitro* activity of FGI-103 against MARV.** Because related viruses may utilize the same or similar host mechanisms, we asked whether FGI-103 might also demonstrate antiviral activity against MARV. We evaluated the activity of FGI-103 against two strains of MARV—MARV-Ravn and MARV-Ci67—by using standard virus yield reduction assays with Vero cells. Cells were pretreated with FGI-103 overnight prior to infection. Cells were infected using an MOI of 1, and FGI-103 was again added to the cell culture medium for 48 h. Virus yield in culture supernatants was quantified using standard plaque assays. Treatment with 25 μM FGI-103 reduced the yield of MARV-Ravn by >3 logs, i.e., >99.9% inhibition (Fig. 2). We observed a dose-dependent inhibition of viral propagation, with antiviral activity apparent at concentrations of >2.5 μM (calculated EC_{50} of 2.5 μM). Similar results were obtained from evaluations using MARV-Ci67. Treatment with 10 μM FGI-103 inhibited the MARV-Ci67 viral yield by >90% (CC_{50} of 2.5 μM). Taken together, these results demonstrate FGI-103 to be a potent inhibitor of filovirus infection, with activity against both EBOV and MARV.

***In vivo* efficacy of FGI-103 against EBOV.** The activity observed in cell-based infection assays was promising but led us to ask if FGI-103 would be effective in animal models of EBOV infection. An evaluation of the acute *in vivo* toxicity of FGI-103 revealed the 50% lethal dose to be in excess of 200 mg/kg when the compound is delivered by the i.p. route (data not shown). We evaluated the efficacy of FGI-103 by using a mouse-adapted strain of EBOV (3), with which our initial studies focused on a prophylactic administration (compound delivered prior to infection). Groups of 10 C57BL/6 mice were injected via the i.p. route on day 0 (1 h prior to infection) and again on days 2 and 5 postinfection with 10 mg/kg FGI-103. Mice were challenged with 1,000 PFU EBOV 1 h after the first injection and were monitored for disease and survival for 14 days. Consistent with previous investigations with this model, a high degree of mortality (90%) was observed in mice treated with the vehicle (Fig. 3A). In contrast, treatment with FGI-103 completely protected mice from lethal EBOV infection. Transient overt manifestations of EBOV infection were noted in five of the FGI-103-treated mice beginning on day 8 postinfection, but the remaining five mice in that treatment group remained outwardly healthy throughout the study and all of the mice were observed to be healthy beginning 10 days following EBOV infection.

The ability to prevent lethal EBOV infection in animal models by prophylactic treatment with FGI-103 was remarkable, but we considered that an effective antiviral would also have utility when administered in a therapeutic (postinfection) setting. To model this scenario, FGI-103 (10 or 5 mg/kg) was delivered to mice by i.p. administration 24 h after mice were infected with EBOV. Animal health and mortality were mon-

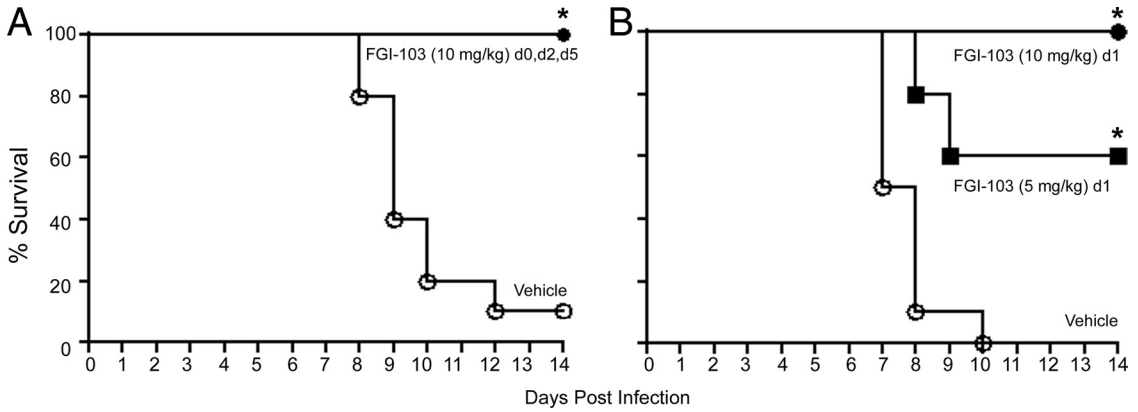

FIG. 3. FGI-103 protects C57BL/6 mice against EBOV infection. Groups of mice ($n = 10$) were challenged with a lethal dose (1,000 PFU) of mouse-adapted ZEBOV delivered by i.p. injection, and animal health and survival were monitored for 14 days. (A) FGI-103 was delivered to mice by i.p. injection as a 10-mg/kg dose in sterile saline. Doses were administered 1 h prior to EBOV infection (d0) and again at days 2 and 5 postinfection. Control mice received treatment with the vehicle according to the same dosing regimen. (B) FGI-103 was administered to mice as either a 10- or a 5-mg/kg dose by a single i.p. injection delivered at day 1 postinfection. Survival curves that differ significantly ($P \leq 0.05$) from that of the vehicle control treatment are indicated by asterisks.

itored for 14 days. Consistent with the previous findings, animals treated with the vehicle succumbed to the infection (Fig. 3B). Mice that were treated with a 10-mg/kg dose of FGI-103 were completely protected following a lethal EBOV challenge. A moderate, but statistically significant, level of protection (60% survival) was observed in mice receiving a 5-mg/kg dose of FGI-103.

We sought to further examine the therapeutic potential of FGI-103 in postexposure scenarios by delivering a single 10-mg/kg dose of FGI-103 1 to 5 days after mice were infected with EBOV. In this experiment, delaying FGI-103 administration 2 days postinfection or later failed to confer a survival advantage relative to the vehicle treatment (data not shown). Taken together, these studies show that a single dose of FGI-103 can effectively protect against EBOV infection when administered via a therapeutic regimen, although the therapeutic window for efficacious treatment with FGI-103 appears to be less than 48 h postinfection.

***In vivo* efficacy of FGI-103 against MARV.** Based on the observed cell-based antiviral activity of FGI-103 against MARV and the encouraging efficacy results obtained in animal-based EBOV challenge experiments, we sought to evaluate whether FGI-103 would protect mice from a lethal challenge with MARV. Mice were treated i.p. either with 5 or 10 mg/kg FGI-103 or with the vehicle only. Treatments were delivered once, 24 h after the mice were infected with 1,000 PFU mouse-adapted MARV. Consistent with expectations, all of the mice treated with the vehicle control succumbed to the infection by 8 days postinfection (Fig. 4). In contrast, mice treated with 10 mg/kg FGI-103 were completely protected against the challenge. Delivery of 5 mg/kg FGI-103 protected 40% of the mice from the lethal MARV challenge. These results clearly demonstrate the potential of FGI-103 as a therapeutic agent to prevent MARV infection in a murine model.

Reduction of viral titer, serum chemistry, inflammatory cytokine response, and histopathology. The pathophysiology of EBOV infection in rodent models has been evaluated in detail and is characterized by viral propagation in the liver, spleen, and kidneys and systemic elaboration of inflammatory cytokines (3, 14). To address this complex set of outcomes, we evaluated the influence of FGI-103 on each of these parameters. Based on compelling evidence that a single dose of FGI-103, administered 1 day postinfection, protects animals from EBOV challenge, this particular experimental protocol was utilized. In addition to the monitoring of overall survival, tissue and serum samples were collected at multiple times postinfection to measure viral burdens, cytokine elaboration, and clinical pathology markers of liver function. In particular, blood chemistry analyses monitored the release of the ALT, AST, and ALP enzymes into serum as an index to EBOV pathoge-

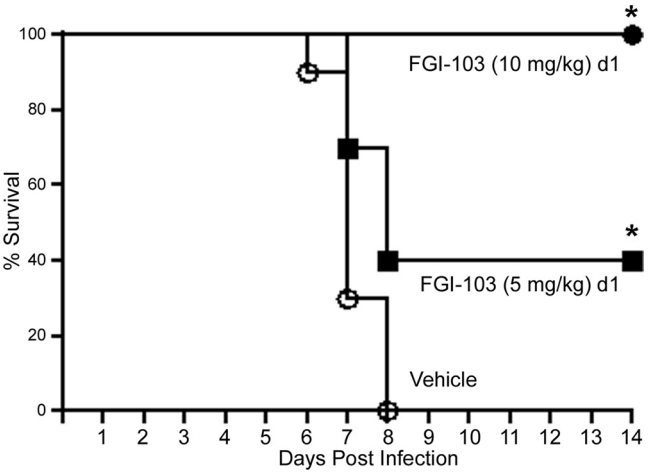

FIG. 4. Delivery of FGI-103 protects BALB/c mice against MARV infection. Mice were challenged with a mouse-adapted strain of MARV-Ravn by delivery of 1,000 PFU by i.p. injection. Treatment groups ($n = 10$) were monitored for 14 days. Doses of FGI-103 (10 or 5 mg/kg) were administered via i.p. injection at day 1 postinfection. Survival curves that differ significantly ($P \leq 0.05$) from that of the vehicle control treatment are indicated by asterisks.

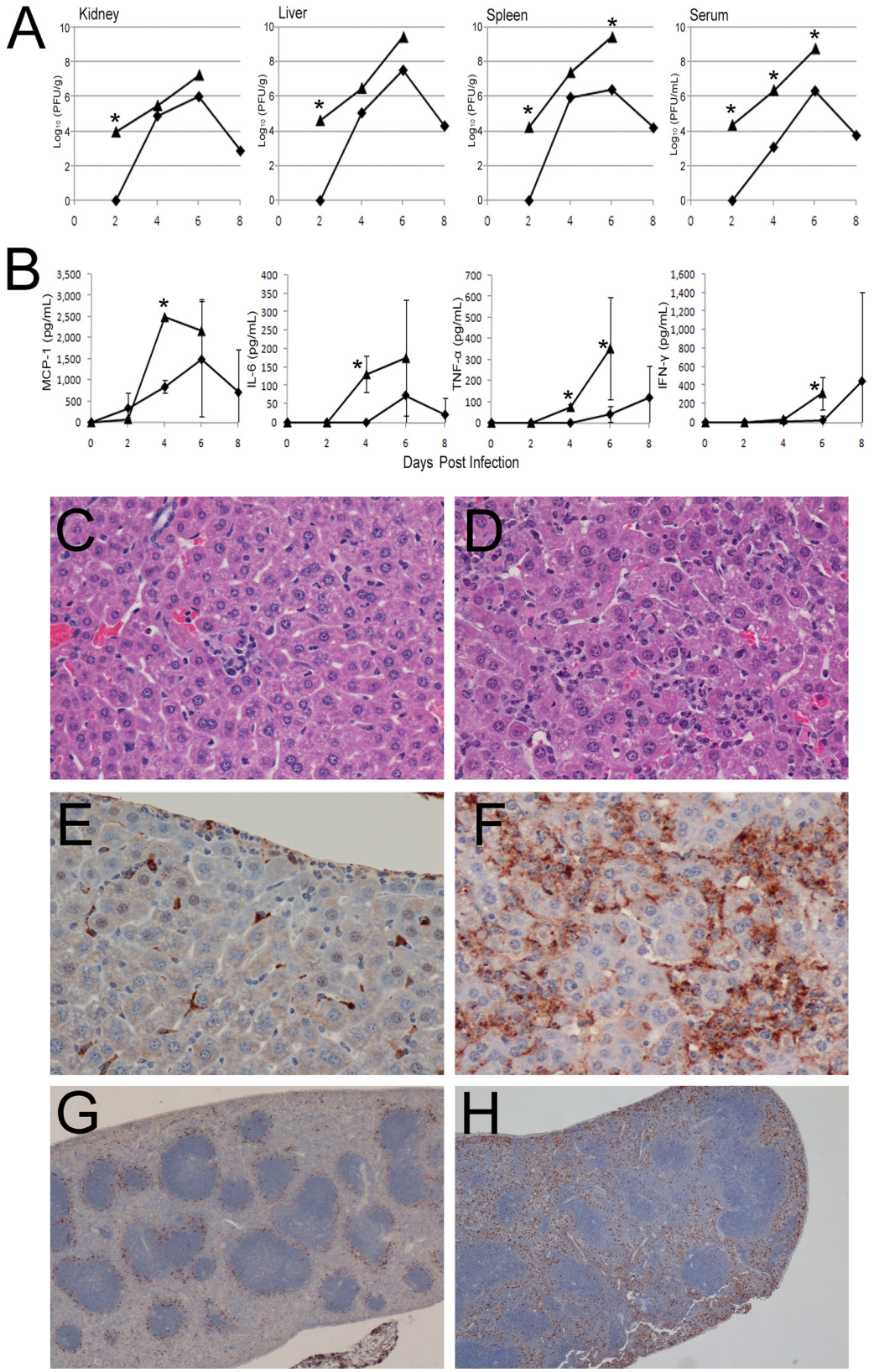

FIG. 5. FGI-103 reduces the *in vitro* EBOV load, proinflammatory cytokine responses, and tissue pathology in mice. C57BL/6 mice were infected with a lethal dose of mouse-adapted ZEBOV (1,000 PFU delivered i.p.). Mice were treated with either FGI-103 (◆) delivered as a single 10-mg/kg dose or with the vehicle (▲) 1 day after infection. Mice ($n = 5$) were sacrificed at the indicated time points to obtain kidney, liver, spleen, and serum samples. Asterisks denote statistically significant ($P \leq 0.05$) differences between the means of vehicle- and FGI-treated mice. (A) Tissue

TABLE 1. Serum liver enzymes in mice following EBOV infection[a]

Days postinfection	ALT (U/liter)			AST (U/liter)			ALP (U/liter)		
	Vehicle	FGI-103	*P* value	Vehicle	FGI-103	*P* value	Vehicle	FGI-103	*P* value
2	18 ± 1.4	148 ± 257	>0.05	83 ± 22	237 ± 341	>0.05	97 ± 15.9	57 ± 6.7	>0.05
4	298 ± 278	23 ± 6.3	<0.05	480 ± 371	54 ± 9.5	<0.05	61 ± 19.5	65 ± 6.4	>0.05
6	>2,000	87 ± 61	<0.05	>2,000	207 ± 81.2	<0.05	249 ± 61.7	67 ± 13.5	<0.05

[a] FGI-103 (10 mg/kg) or vehicle was delivered to mice by i.p. injection 24 h following infection with a lethal dose (1,000 PFU) of mouse-adapted ZEBOV. Values represent the mean ± standard deviation of values obtained from five animals. Statistical analysis was not performed when all values for a treatment exceeded the range of detection.

nicity. Additionally, multiple organs were preserved for histological examination.

Consistent with the aforementioned studies, assessments of overall survival demonstrated that FGI-103 protected animals from an otherwise lethal challenge. Whereas all but one animal that received FGI-103 survived throughout the study (at least 14 days), none of the animals treated with the vehicle survived for more than 8 days postinfection. This outcome provided a foundation to ask what parameters might relate to survival as an outcome. Using the serum and tissue samples harvested at specified time points after infection, the EBOV burden was determined by using standard plaque assays. These studies detected EBOV in vital organs (kidneys, liver, and spleen) and in serum within 2 days in vehicle-treated control animals (Fig. 5A). In control animals, the levels of EBOV steadily increased throughout the study in all organs until the time of death. FGI-103 treatment delayed the time at which EBOV was detected, and while the viral burden increased over time in FGI-103-treated mice, the levels were often reduced by 1 to 2 logs (10- to 100-fold) compared with those in control animals. In FGI-103-treated animals, the viral burden peaked 6 days after infection and decreased thereafter, which is consistent with resolution of the disease in the FGI-103-treated survivors.

We then evaluated pathophysiological parameters to identify potential markers of FGI-103 efficacy. It is generally understood that filovirus infection triggers an inflammatory cascade, known as a cytokine storm, which is thought to contribute substantially to the morbidity and mortality of EBOV infection. Therefore, we evaluated the circulating levels of a panel of inflammatory cytokines, with particular emphasis upon monocyte chemoattractant protein 1 (MCP-1), tumor necrosis factor α (TNF-α), and interleukin-6 (IL-6), secreted factors to which prominent roles in EBOV pathology have been attributed (10, 14). In vehicle-treated controls, high levels of MCP-1 and IL-6 levels were observed 2 to 3 days prior to death (Fig. 5B). In contrast, the levels of these cytokines were markedly lower in FGI-103-treated animals and never achieved the levels observed in vehicle-treated animals.

High levels of inflammatory cytokines can harm vital organs, including the liver and kidneys. Therefore, we asked if markers of liver toxicology might convey information about FGI-103 efficacy. Indeed, high levels of all three liver markers (ALT, ALP, and AST) were observed in vehicle-treated controls on day 6, just prior to the onset of EBOV-mediated death (Table 1). In contrast, the levels of these markers in FGI-103-treated subjects remained at comparatively low levels at this time. While a transient elevation of mean serum ALT and AST values was observed in FGI-103-treated mice ($n = 5$) at day 2 postinfection (24 h following compound administration), it is important to note that elevated enzyme levels were noted in only one animal and that normal enzyme levels were observed in the remaining four FGI-103-treated mice sampled at that time point.

Histopathological examination of tissues from vehicle-treated mice revealed mild hepatitis with hepatocellular necrosis in the liver and lymphocytolysis in the spleen, conditions consistent with EBOV infection, at 4 days postinfection in both vehicle- and FGI-103-treated mice (not shown). These conditions had increased in severity in vehicle-treated mice by 6 days postinfection but remained mild in mice treated with FGI-103 (Fig. 5C and D). Viral antigen was prevalent in liver and spleen tissues from vehicle-treated mice at 6 days postinfection, while the presence of viral antigen in liver and spleen tissues from FGI-103-treated mice was confined primarily to Kupffer cells in the liver and to the periphery of lymphatic nodules in the spleen (Fig. 5E to H). These results corroborate the viral titers in the spleen and liver, which showed a reduction in viral burden in these tissues in mice treated with FGI-103.

DISCUSSION

We used a recombinant, GFP-expressing strain of EBOV to conduct a high-throughput screen of nonpeptidic small-mole-

samples were homogenized and subjected to a standard plaque assay using Vero cells. The median values of five samples are displayed. (B) Serum cytokine concentrations were determined using a BD Cytometric Bead Array according to the manufacturer's instructions. Average serum cytokine concentrations are shown, and error bars represent standard deviations. (C and D) Representative images of hematoxylin-and-eosin-stained liver tissue (×600) collected at day 6 postinfection showing mild necrosis and hepatitis in the FGI-103-treated animal (C) with more progressive pathology in the vehicle-treated mouse (D). (E to H) Immunoperoxidase staining of tissue collected at day 6 postinfection showing viral antigen in brown with hematoxylin counterstain. In liver tissue (×600) from FGI-103-treated mice (E), the viral antigen is apparently localized to Kupffer cells, while in mice treated with the vehicle (F), the viral antigen is more prevalent and distributed throughout the liver. (G and H) Comparison of viral antigen in spleen tissue (×100) collected from FGI-103-treated animals (G) and vehicle-treated mice (H).

cule compound libraries. From this effort, we identified FGI-103 as a potent inhibitor of ZEBOV-GFP, and additional cell-based evaluations showed FGI-103 to be capable of inhibiting the replication of wild-type ZEBOV and SEBOV, as well as multiple strains of MARV. Evaluated in animal-based models of filovirus infection, administration of a single 10-mg/kg dose of FGI-103, administered therapeutically (i.e., 24 h following challenge), completely protected mice against an otherwise lethal challenge with ZEBOV or MARV. Similarly, mice were completely protected against a lethal EBOV challenge when FGI-103 was delivered prior to infection and again on days 2 and 5 postinfection. Taken together, these results suggest the potential to develop a much-needed treatment for filovirus infection and that FGI-103 could have applications for both prophylactic (e.g., to protect first-responder emergency workers or medical personnel attending potentially infected patients) and therapeutic cases of known or suspected exposure.

The mechanistic basis of FGI-103 antiviral activity is largely unknown. Our findings suggest that FGI-103 prevents EBOV-mediated liver damage, perhaps by preventing insult caused by direct viral propagation or subsequent cytokine responses. Based on evidence that FGI-103 can block viral propagation in cell-based models, this outcome likely does not represent an indirect effect of FGI-103 on cytokine levels (although this possibility cannot be ruled out based on the available data) but instead implies a direct effect on viral infection or propagation. The mechanistic basis of FGI-103 activity may involve antiviral activity at a relatively late stage of the EBOV life cycle. This idea is supported by evidence that FGI-103 does not interfere with the transduction of pseudotyped virus into host cells (not shown) and that it does not interfere with replication of the EBOV minigenome replicon (not shown). Thus, we postulate that FGI-103 impacts a stage of the viral life cycle that is downstream of nucleic acid replication. Studies to evaluate this in greater detail are ongoing in our laboratories.

We have shown previously that EBOV utilizes the host vacuolar protein sorting (vps) machinery in general for efficient budding (17, 18). A component of the vps system, TSG101, has been shown to be involved with both EBOV (15, 17)- and MARV (22)-derived VP40 to mediate viral budding and release. Recently, a broad-spectrum small-molecule inhibitor of EBOV, FGI-104, has been described, and TSG101 was reported as a possible molecular target (11). To ask if TSG101 might be targeted by FGI-103, the interaction of EBOV VP40 and TSG101 was modeled using a solid-phase assay in which His-tagged TSG101 was immobilized on enzyme-linked immunosorbent assay plates via an anti-His tag. These analyses indicate that FGI-103 does not interfere with TSG101-VP40 binding (not shown). Investigations are currently ongoing to determine if FGI-103 interferes with virion egress from infected cells in a manner independent of TSG-101.

An alternative explanation for the observed potency of FGI-103 is that the drug achieves concentrations that inhibit, or alter the functionality of, cells that are initially infected by and disseminate filoviruses. Investigations of Gibb et al. (9) have shown that mouse-adapted ZEBOV initially (at day 2 postinfection) infects and replicates in macrophage/monocyte cells of lymph nodes, and by day 3 postinfection, large numbers of monocytes and macrophages, as well as hepatocytes, are infected. It is thus conceivable that FGI-103 alters the functionality of macrophages or monocytes to create conditions inhospitable for viral replication and spread during the initial days of infection. Viral titer data from FGI-103-treated infected mice demonstrate that viral replication is reduced as early as day 2 postinfection, within 24 h following compound administration (Fig. 5A). Perhaps this delay in viral replication tips the balance in favor of the host by providing time for the development of antigen-specific immunogenic responses, which would normally become overwhelmed by unabated viral replication in untreated hosts. We have observed that serum levels of TNF-α, which is primarily produced by macrophages, are reduced in mice treated with FGI-103 (Fig. 5B), perhaps indicating suppressed macrophage functionality. However, it is also possible that the reduced severity of infection conferred by macrophage-independent mechanisms in FGI-103-treated mice results in lower TNF-α secretion by macrophages. Further studies are required to determine whether FGI-103 alters the function of macrophages or monocytes.

Although FGI-103 has shown potent antiviral activity against EBOV and MARV, we cannot exclude the possibility that additional, as-yet-unrecognized, mechanisms—such as stimulation of innate immunogenic responses—contribute to the efficacy of this compound. Bray et al. reported that administration of the adenosine analog 3-deazaneplanocin A protects mice against a lethal challenge with mouse-adapted ZEBOV following a single 1-mg/kg dose by inducing a massive alpha interferon (IFN-α) response in EBOV-infected cells (4, 5). Interestingly, 3-deazaneplanocin A induced a poor type I IFN response in uninfected cells and in mice that had not been infected with ZEBOV. Our investigations have shown no evidence that uninfected human peripheral blood mononuclear cells produce IFN-α in response to FGI-103 (not shown). A finding that FGI-103 induces a type I IFN response in filovirus-infected cells would help explain its efficacy but would suggest that its antiviral activity is exerted by a separate mechanism in assays containing Vero cells, which have impaired IFN production capability (8). Whether FGI-103 induces the production of other antiviral cytokines remains to be investigated.

We recently reported the discovery of a small-molecular antiviral compound, FGI-106, which, similar to FGI-103, also provides a high degree of protection to mice in an EBOV infection model following the delivery of a single dose (1). Additionally, protective efficacy against EBOV in mice has been described for a third small molecule, FGI-104 (11). Despite their similar efficacy profiles, it is important to emphasize that the chemical structures of these compounds are distinct. While the broad-spectrum antiviral activity of FGI-104 and FGI-106 has been documented, our studies demonstrating efficacy of FGI-103 against both EBOV and MARV in infected mice have produced novel findings.

Recent findings that EBOV-Reston infects pigs and has potentially infected humans in the Philippines (2, 16) suggest that filoviruses may be more widespread than has been recognized and further highlight the urgent need for the development of effective therapeutics to combat filovirus disease. Our current research efforts aim to characterize and develop FGI-103 to determine optimal delivery formulations and routes of administration; fully characterize the pharmacokinetic, pharmacodynamic, and toxicological properties of FGI-103; and

assess its mechanism of antiviral activity in murine and nonhuman primate models in order to find effective approaches to therapeutic intervention during human filovirus infections.

ACKNOWLEDGMENTS

The research described herein was sponsored by the Transformation Medical Technologies Initiative of the Defense Threat Reduction Agency (contracts HDTRA1-07-C-0080 and 4.10039_07_RD_B) and the Medical Research and Material Command.

We acknowledge Sean Van Tongeren, Kelly Donner, Cary Retterer, and Nicole Garza for their excellent technical assistance.

The opinions, interpretations, conclusions, and recommendations in this report are ours and are not necessarily endorsed by the U.S. Army.

REFERENCES

1. **Aman, M. J., M. S. Kinch, K. Warfield, T. Warren, A. Yunus, S. Enterlein, E. Stavale, P. Wang, S. Chang, Q. Tang, K. Porter, M. Goldblatt, and S. Bavari.** 2009. Development of a broad-spectrum antiviral with activity against Ebola virus. Antiviral Res. **83:**245–251.
2. **Anonymous.** 2009. Ebola Reston in pigs and humans, Philippines. Wkly. Epidemiol. Rec. **84:**49–50.
3. **Bray, M., K. Davis, T. Geisbert, C. Schmaljohn, and J. Huggins.** 1998. A mouse model for evaluation of prophylaxis and therapy of Ebola hemorrhagic fever. J. Infect. Dis. **178:**651–661.
4. **Bray, M., J. Driscoll, and J. W. Huggins.** 2000. Treatment of lethal Ebola virus infection in mice with a single dose of an *S*-adenosyl-L-homocysteine hydrolase inhibitor. Antiviral Res. **45:**135–147.
5. **Bray, M., J. L. Raymond, T. Geisbert, and R. O. Baker.** 2002. 3-Deazaneplanocin A induces massively increased interferon-alpha production in Ebola virus-infected mice. Antiviral Res. **55:**151–159.
6. **Centers for Disease Control and Prevention.** 2005. Outbreak of Marburg virus hemorrhagic fever—Angola, October 1, 2004-March 29, 2005. MMWR Morb. Mortal. Wkly. Rep. **54:**308–309.
7. **Dolnik, O., L. Kolesnikova, and S. Becker.** 2008. Filoviruses: interactions with the host cell. Cell. Mol. Life Sci. **65:**756–776.
8. **Emeny, J. M., and M. J. Morgan.** 1979. Regulation of the interferon system: evidence that Vero cells have a genetic defect in interferon production. J. Gen. Virol. **43:**247–252.
9. **Gibb, T. R., M. Bray, T. W. Geisbert, K. E. Steele, W. M. Kell, K. J. Davis, and N. K. Jaax.** 2001. Pathogenesis of experimental Ebola Zaire virus infection in BALB/c mice. J. Comp. Pathol. **125:**233–242.
10. **Hensley, L. E., H. A. Young, P. B. Jahrling, and T. W. Geisbert.** 2002. Proinflammatory response during Ebola virus infection of primate models: possible involvement of the tumor necrosis factor receptor superfamily. Immunol. Lett. **80:**169–179.
11. **Kinch, M. S., A. S. Yunus, C. Lear, H. Mao, H. Chen, Z. Fesseha, G. Luo, E. A. Nelson, L. Li, Z. Huang, M. Murray, W. Y. Ellis, L. E. Hensley, J. Christopher-Hennings, G. G. Olinger, and M. Goldblatt.** 2009. FGI-104: a broad-spectrum small molecule inhibitor of viral infection. Am. J. Transl. Res. **1:**87–98.
12. **Kortepeter, M. G., J. W. Martin, J. M. Rusnak, T. J. Cieslak, K. L. Warfield, E. L. Anderson, and M. V. Ranadive.** 2008. Managing potential laboratory exposure to Ebola virus by using a patient biocontainment care unit. Emerg. Infect. Dis. **14:**881–887.
13. **Kuhn, J. H.** 2008. Filoviruses: a compendium of 40 years of epidemiological, clinical, and laboratory studies. Springer, New York, NY.
14. **Mahanty, S., M. Gupta, J. Paragas, M. Bray, R. Ahmed, and P. E. Rollin.** 2003. Protection from lethal infection is determined by innate immune responses in a mouse model of Ebola virus infection. Virology **312:**415–424.
15. **Martin-Serrano, J., T. Zang, and P. D. Bieniasz.** 2001. HIV-1 and Ebola virus encode small peptide motifs that recruit Tsg101 to sites of particle assembly to facilitate egress. Nat. Med. **7:**1313–1319.
16. **Normile, D.** 2009. Emerging infectious diseases. Scientists puzzle over Ebola-Reston virus in pigs. Science **323:**451.
17. **Panchal, R. G., G. Ruthel, T. A. Kenny, G. H. Kallstrom, D. Lane, S. S. Badie, L. Li, S. Bavari, and M. J. Aman.** 2003. In vivo oligomerization and raft localization of Ebola virus protein VP40 during vesicular budding. Proc. Natl. Acad. Sci. U. S. A. **100:**15936–15941.
18. **Silvestri, L. S., G. Ruthel, G. Kallstrom, K. L. Warfield, D. L. Swenson, T. Nelle, P. L. Iversen, S. Bavari, and M. J. Aman.** 2007. Involvement of vacuolar protein sorting pathway in Ebola virus release independent of TSG101 interaction. J. Infect. Dis. **196**(Suppl. 2)**:**S264–S270.
19. **Streeter, D. G., J. T. Witkowski, G. P. Khare, R. W. Sidwell, R. J. Bauer, R. K. Robins, and L. N. Simon.** 1973. Mechanism of action of 1-D-ribofuranosyl-1,2,4-triazole-3-carboxamide (Virazole), a new broad-spectrum antiviral agent. Proc. Natl. Acad. Sci. U. S. A. **70:**1174–1178.
20. **Timen, A., M. P. Koopmans, A. C. Vossen, G. J. van Doornum, S. Gunther, F. van den Berkmortel, K. M. Verduin, S. Dittrich, P. Emmerich, A. D. Osterhaus, J. T. van Dissel, and R. A. Coutinho.** 2009. Response to imported case of Marburg hemorrhagic fever, the Netherlands. Emerg. Infect. Dis. **15:**1171–1175.
21. **Towner, J. S., J. Paragas, J. E. Dover, M. Gupta, C. S. Goldsmith, J. W. Huggins, and S. T. Nichol.** 2005. Generation of eGFP expressing recombinant Zaire ebolavirus for analysis of early pathogenesis events and high-throughput antiviral drug screening. Virology **332:**20–27.
22. **Urata, S., T. Noda, Y. Kawaoka, S. Morikawa, H. Yokosawa, and J. Yasuda.** 2007. Interaction of Tsg101 with Marburg virus VP40 depends on the PPPY motif, but not the PT/SAP motif as in the case of Ebola virus, and Tsg101 plays a critical role in the budding of Marburg virus-like particles induced by VP40, NP, and GP. J. Virol. **81:**4895–4899.
23. **Warfield, K. L., D. A. Alves, S. B. Bradfute, D. K. Reed, S. VanTongeren, W. V. Kalina, G. G. Olinger, and S. Bavari.** 2007. Development of a model for marburgvirus based on severe-combined immunodeficiency mice. Virol. J. **4:**108.
24. **Warfield, K. L., S. B. Bradfute, J. Wells, L. Lofts, M. T. Cooper, D. A. Alves, D. K. Reed, S. A. VanTongeren, C. A. Mech, and S. Bavari.** 2009. Development and characterization of a mouse model for Marburg hemorrhagic fever. J. Virol. **83:**6404–6415.